# FAILURE PROBABILITY ANALYSIS OF OVERHEAD CRANE BRIDGE GIRDERS WITHIN UNCERTAIN DESIGN PARAMETERS

Trinh Van Hai[a,*], Nguyen Huu Thu[a], Ha Dang Tuan[a], Pham Van Hiu[a]

[a]*Faculty of Vehicle and Energy and Engineering (FVEE), Le Quy Don Technical University, 236 Hoang Quoc Viet street, Bac Tu Liem district, Hanoi, Vietnam*

## Abstract

In the design of steel crane girders, various sources of uncertainty such as material properties, loads, and geometric tolerances are inherent and inevitable. Using deterministic structural and/or load conditions may lead to low-reliability systems in real applications. In this paper, the probability of failure of overhead crane bridge girders with uncertain design parameters is investigated. First, the design problem of a crane double girder is introduced within a set of analytical stress and defection constraints. Then, the response surface method is used in conjunction with Monte Carlo methods to quantify the effect of the parameter uncertainties on the constraints of stress and deflection. For illustrative examples, various configurations of girders with original deterministic parameters proposed in the literature are selected and their deterministic optimization values are considered as the mean of random variables. The obtained results reveal that uncertainties such as coefficients of variation (COV) in structures and loads have strong effects on the probability of failure for all stated crane girder configurations. For only a wheel load COV of 0.05 and geometric dimension COV of 0.025, the means of geometric parameters have to be larger than 1.1 their deterministic-based values in order to reach a probability of failure at a level of $10^{-4}$.

*Keywords:* failure probability; double-box girder; overhead crane; Monte Carlo method.

## 1. Introduction

Cranes are widely used for moving, lifting, and handling tasks in various industrial fields, such as construction and manufacturing [1, 2]. According to their primary dynamic properties and structural characteristics, cranes can mainly be classified into three types: overhead crane, mobile crane, and tower crane. An overhead traveling crane consists of three independent motions (i.e. hosting, long travel, and cross travel), which allow handling and transferring payloads from one position to another in the working space within its own traveling and hoisting. As a wide application and multi-functional purposes, overhead cranes are the primary equipment in the area of transport and handling machinery [1].

Cranes are widely used for moving, lifting, and handling tasks in various industrial fields, such as construction and manufacturing [1, 2]. According to their primary dynamic properties and structural characteristics, cranes can mainly be classified into three types: overhead crane, mobile crane, and

*Corresponding author. E-mail address:* hai.tv@lqdtu.edu.vn (Hai, T. V.)

tower crane. An overhead traveling crane consists of three independent motions (i.e. hosting, long travel, and cross travel), which allow handling and transferring payloads from one position to another in the working space within its own traveling and hoisting. As a wide application and multi-functional purposes, overhead cranes are the primary equipment in the area of transport and handling machinery [1].

The main task during the design process of a bridge crane structure is to optimize the shape and dimensions of the main girder. In terms of deterministic-based design, different methods have been proposed to archive the geometric parameters of the rectangular hollow section of the girder that has a minimum area [3, 4]. Currently, these optimization methods mainly include finite element method (FEM) [5, 6], neural networks [7, 8], Lagrange multipliers [9, 10], amongst others [11, 12]. However, these methods are all based on deterministic optimum designs without considering effects of randomness or uncertainties in the structure parameters and/or load conditions. Deterministic optimum designs, which are pushed to the limits of their constraint boundaries and have no room for uncertainty, may result in low-reliability designs [13, 14]. Recently, reliability-based design problems of crane structure have been reported in a few reference works [15]. Using the FEM simulations and response surface method (RSM), a reliability-based design of the structure of tower crane was introduced in Ref. [16]. A neural network model based on finite element and first-order second-moment (FOSM) method is used to investigate the reliability and sensitivity of crane steel structure [17].

Structural reliability can be analyzed using analytical methods, such as FOSM and second-order second moments (SOSM) or with simulation methods such as Monte Carlo (MC) method [18, 19]. The FOSM method is very simple and requires minimal computation effort but sacrifices accuracy for nonlinear limit state functions. The accuracy of the SOSM method is improved compared with that of the FOSM [20]. However, SOSM method is not widely used due to demanding computational costs. MC method seems to be a computationally intensive option when requiring a large number of samples to evaluate small failure probabilities (e.g., for multi-scale FEM computations in high-dimensional problems), but it is accurate for cases of large samplings available based on analytical or surrogate models [21].

In this work, the design problem of a crane double girder is introduced within a set of analytical stress and defection constraints. The response surface method is then used in conjunction with the MC method to quantify the effect of the parameter uncertainties on the proposed constraints in order to estimate the failure probability of girder designs.

## 2. Formulations of girder design problem

### 2.1. Overhead crane and its girder structure

In this study, we consider a configuration of double girder overhead cranes, that makes up of two box-type bridge girders, two end trucks or end girders, and a trolley hoist assembly (Fig. 1(a)). The trolley hoist handling hook loads travels on top of rails that are mounted or welded to the top of the bridge girders. For a sake of simplicity, the cross-section of the girder (as shown in Fig. 1(c)) is assumed constant throughout its span, and the rail and the stiffeners are neglected in the calculation of the cross-sectional characteristics.

Fig. 1(b) shows the calculation schema for modeling a double girder of overhead cranes. This simplified model consists of a simple-span beam with a length of $L$. For single girder, two-wheel loads $F$ are equal to a quarter of the total of the trolley mass $G_t$ and the service load $H$. The linear distributed masses $q$ represents the self-weight of the girder and the additional distributed masses

(like rails and the sidewalk). Noted that the wind load, buffer loads, and skew loads due to travelling are not considered here.

### 2.2. Constraint functions

The static problem for designing a crane structure has been proposed in a number of studies. Herein, we focus on three design constraints as follows [3]:

**Constraint on the static stress in the lower flange**

The constraint on the static stress in the lower flange at mid-span due to biaxial bending is:

$$\sigma_s = \frac{M_x}{W_x} + \frac{M_y}{W_x} \leq \bar{\sigma}_s \tag{1}$$

where $M_x$ and $M_y$ are the bending moments, $W_x$ and $Wy$ are the section moduli. $\bar{\sigma}_s$ is the allowable stress estimated as $\bar{\sigma}_s = \alpha_d(\alpha_s Y_s)$ where $Y_s$ is the yield stress, $\alpha_d$ is the duty factor, and $\alpha_s = 0.59$ [3, 22].

The moments of inertia are calculated as,

$$I_x = \frac{t_w h^3}{6} + 2\left[\frac{(b + 2d) t_f^3}{12} + \left(\frac{h}{2} + \frac{t_f}{2}\right)^2 (b + 2d) t_f\right]$$

$$I_y = \frac{t_f(b + 2d)^3}{6} + 2\left[\frac{ht_w^3}{12} + \left(\frac{b}{2} - \frac{t_w}{2}\right)^2 ht_w\right] \tag{2}$$

The section moduli are:

$$W_x = \frac{2I_x}{h + 2t_f}; \quad W_y = \frac{2I_y}{b + 2d} \tag{3}$$

The bending moment due to vertical loads is given as,

$$M_x = \frac{L^2 q}{8} + \frac{\psi_d H + G_t}{8L}\left(L - \frac{k}{2}\right)^2 \tag{4}$$



(a) Structure of a overhead crane

(b) Simplified model of crane girder

(c) Girder cross-section
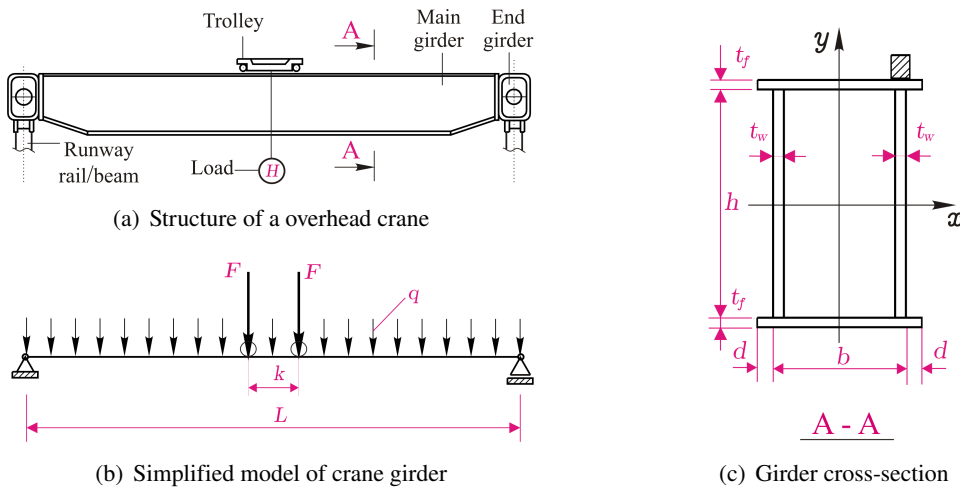
Figure 1. Crane configuration and calculation schema of its girder

where $(\psi_d H + G_t)/4$ is the wheel load, $q = \left(k_g A\rho + p_r + p_s\right)g$ is the linear distributed weight with $k_g A\rho$ is girder distributed mass within considering stiffeners and diaphragms by a factor of $k_g = 1.05$, and $A = 2\left[ht_w + (b + d)t_f\right]$ is the girder cross-sectional area given. $k$ is the distance between the trolley axes, $g = 10$ m/s$^2$, and $\rho = 7850$ kg/m$^3$.

The bending moment due to horizontal loads is given as,

$$M_y = k_M \left[\frac{L^2 q}{8} + \frac{G_t}{8L}\left(L - \frac{k}{2}\right)^2\right] \tag{5}$$

where $k_M = 0.3 \times 0.5$ with a factor of 0.3 represents the effect of inertia forces, and a factor of 0.5 recognizes that two of four trolley wheels are driven [3].

***Constraint on fatigue stress***

Based on the fatigue failure theory, the constraint on fatigue stress in the lower flange at mid-span may be given as [3],

$$\sigma_f = \frac{M_{xf}}{W_x} + \frac{M_y}{W_x} \leq \bar{\sigma}_f \tag{6}$$

where $\bar{\sigma}_f$ is the permissible tensile fatigue stress depending on the number of cycles NG and the ratio $f_\sigma$ between the minimum and the maximum stress, $f_\sigma \approx M_{x1}/M_x$ with $M_{x1} = L^2 q/8$. The approximate formulas to calculate $\bar{\sigma}_f$ are presented in Table 2. The moment $M_{xf}$ due to fatigue is expressed as,

$$M_{xf} = \frac{L^2 q}{8} + \frac{K_p \psi_d H + G_t}{8L}\left(L - \frac{k}{2}\right)^2 \tag{7}$$

where $K_p$ is the spectrum factor.

***Constraint on static deflection***

The maximum deflection due to all considered loads is estimated as,

$$w_p = \frac{(H + G_t)(L - k)}{192EI_x}\left[3L^2 - (L - k)^2\right] + \frac{5qL^4}{384EI_x} \leq \bar{w}_p \tag{8}$$

in which $\bar{w}_p$ is the permissible deflection.

## 3. Formulation of structural reliability analysis

### 3.1. Definition of reliability

Time-independent reliability is often used in the design of civil structural systems under various uncertainty sources. This definition can estimate the probability that the actual performance of an engineering system meets the required or specified design performance. By modeling uncertainty sources as random variables, the time-independent reliability $R(\mathbf{X})$ can be formulated as,

$$R(\mathbf{X}) = P(G(\mathbf{X}) \geq 0) = 1 - P(G(\mathbf{X}) < 0) \tag{9}$$

where the random vector $\mathbf{X} = [X_1, X_2, \ldots, X_n]^T$ presents uncertainty sources, $G(\mathbf{X})$ is a system performance function, and $P(\mathbf{E})$ is the probability of the event $\mathbf{E}$. The uncertainties in vector $\mathbf{X}$ further propagate and lead to the uncertainty of the system performance function $G$. In reliability analysis, equation $G(\mathbf{X}) = 0$ is called the limit-state function, which divides the working space into the safety region $G(\mathbf{X}) \geq 0$ and the failure region $G(\mathbf{X}) < 0$.

Consider the safety margin between the strength **S** of an engineered system and the load **L** on this system. This well-known performance function takes the following form,

$$G = \mathbf{S} - \mathbf{L} \tag{10}$$

The strength **S** and load **L** are random in nature, and their randomness can be characterized respectively by the probability density function (PDF) $f_S(\mathbf{S})$ and $f_L(\mathbf{L})$. Fig. 2(a) shows these PDFs for a case of normal distribution. The probability of failure depends on the intersection area of the two PDFs, where the load on the system might exceed its strength. In Fig. 2(b), the probability of failure is indicated by the shaded area. Noted that the distance between the mean performance function $\mu_G$ and the limit state $G = 0$ is equal to the standard deviation $\sigma_G$ multiplied by a factor $\beta$ named the reliability index. In reliability analysis, this factor is calculated as,

$$\beta = \Phi^{-1}(R) \tag{11}$$



(a) Distributions of load and strength          (b) Probability of failure
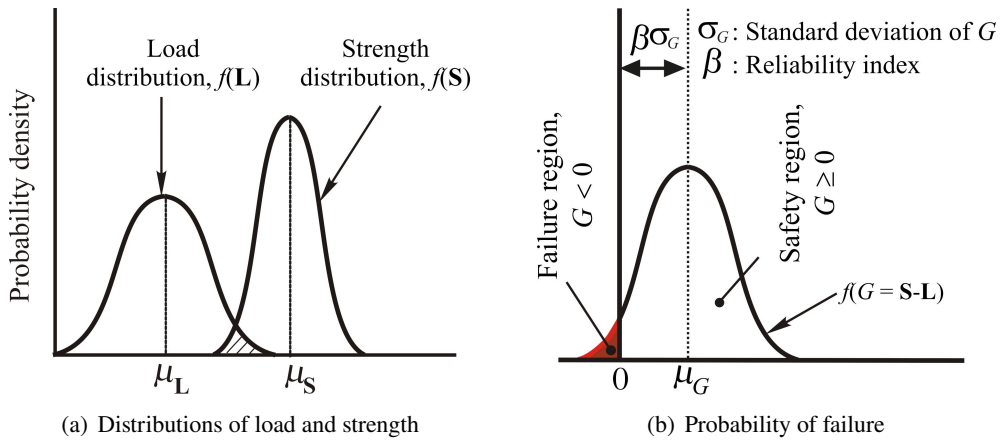
Figure 2. Probabilistic design concept

For the girder design problem mentioned above, the corresponding performance functions of three independent constraints can be expressed as,

$$\begin{cases} G_1 = \bar{\sigma}_s - \sigma_s \\ G_2 = \bar{\sigma}_f - \sigma_f \\ G_3 = \bar{w}_p - w_p \end{cases} \tag{12}$$

### 3.2. Monte Carlo approach

Typically, MC method involves the analysis of a large number of simulations of an analytical or numerical system model. The MC approach considers functions given as $\mathbf{Y} = \mathbf{\Gamma}(\mathbf{X})$, in which $\mathbf{\Gamma}$ represents the model under consideration, $\mathbf{X}$ is a vector of uncertain input variables, $\mathbf{X} = [H \; Y_s \; h \; t_w \; b \; t_f]^T$, and $\mathbf{Y}$ is a vector of estimated outputs, $\mathbf{Y} = [\sigma_s \; \sigma_f \; w_p]^T$. A general procedure of the MC approach is introduced as follows:

(i) Construct a vector $\mathbf{X}$ consisting of 6 relevant input parameters. Here, the probability distribution for each input parameter is generated based on the normal distribution.

(ii) Generate a sample value for each of the 6 input variables. Specifically, a sample of $X_j = [X_{j1}, X_{j2}, \ldots, X_{j6}]$ is generated from the input parameter space.

(iii) Evaluate the output response from an analytical model using the input parameter values $X_j$ as model parameter values.

(iv) Repeat steps (ii) and (iii) to generate a distribution for the output metric. For a stable convergence of output distribution, the number of simulations $N$ is chosen to be large enough. Then, the probability distribution of the output metric can be determined, and its statistics (e.g., mean $E$, standard deviation $D$, Skewness $Sk$, and Kurtosis $Ku$) can be calculated:

$$
\begin{aligned}
E(Y) &= \frac{1}{N} \sum_{i=1}^{N} \Gamma(X_i) \\
D(Y) &= \sqrt{\frac{1}{N} \left[ \sum_{i=1}^{N} \Gamma(X_i) - E(Y) \right]^2} \\
Sk &= \frac{1}{N} \sum_{i=1}^{N} \left[ \frac{\Gamma(X_i) - E(Y)}{D(Y)} \right]^3 \\
Ku &= \frac{1}{N} \sum_{i=1}^{N} \left[ \frac{\Gamma(X_i) - E(Y)}{D(Y)} \right]^4
\end{aligned}
\tag{13}
$$

The probability of the failure can be mathematically defined by,

$$
P_f = \int \cdots \iint \mathbf{I(X)} f_x(\mathbf{X}) d\mathbf{X}
\tag{14}
$$

where $f_x(\mathbf{X})$ is the probability density function of $\mathbf{X}$ and $\mathbf{I(X)}$ is the indicator function defined as,

$$
\mathbf{I(X)} = \begin{cases} 1 & \text{if } \mathbf{X} \text{ is in the failure region } (\text{e.g., } G(\mathbf{X}) < 0) \\ 0 & \text{otherwise} \end{cases}
\tag{15}
$$

Eq. (13) shows that the failure probability is indeed the mean value of the indicator function $\mathbf{I(X)}$, which can thus be estimated as,

$$
P_f = \frac{1}{N} \sum_{i=1}^{N} \mathbf{I}(X_i)
\tag{16}
$$

where $X_i$ denotes the $i$th sample of $\mathbf{X}$ in the sampling $N$.

## 4. Results and discussion

### 4.1. Illustrative girder configurations

To carry out the aim of this study, various reference configurations of girders proposed in Table 2 of Ref. [3] are selected. The original deterministic parameters of these crane girders are tabulated in Table 1. For the name of girders listed in the first column, the prefixes L-, H-, and M- indicate respectively the Light, Moderate, and Heavy loading states, whereas the suffixes -1, -2, and -3 correspond three levels of the steel strength ($Y_s = 230/355/450$ N/mm$^2$).

The present work uses the following deterministic data [3]: $L = 22.5$ m, $G_t = 42.25 \times 10^3$ N, $p_r + p_s = 190$ kg/m, $E = 2.1 \times 10^6$ N/mm$^2$, $d = 10$ mm. Others ($H, Y_s, h, t_w, b, t_f$) are considered as normal random variables with their mean $\mu_i$ and coefficients of variation COV$_i$. We select $\mu_H = 200 \times 10^3$ N, $\mu_{Y_s} = 230/355/450$ N/mm$^2$, and $\mu_x = k^{geo} x^{op}$ with four remaining geometric parameters, whereas coefficients of variation COV$_F$ and COV$_{geo}$ for ($H, Y_s$) load and ($h, t_w, b, t_f$) geometry factors are chosen as tuned factors.

### 4.2. Reliability analysis of girder design

First, the uncertainty of load and geometric parameters is given with $COV_F = 0.05$, $COV_{geo} = 0.025$, and $k_{geo} = 1.05$. The probability statistics of the working static stress, fatigue stress, and static deflection are depicted in Table 3 (herein, $N = 10^6$ for all MC simulation samplings). Generally, the obtained results reveal that three working parameters have the same normal distribution (e.g., factor *Sk* is in range of 0.15 to 0.24, and factor *Ku* is in range of 3.04 to 3.12). This means that these output metrics have the same distribution function compared to the input uncertain variables.

For sake of clear visibility of the state limit function, the distribution functions of working and permissible parameters are demonstrated. As an example, Fig. 3(a) and 3(b) show the PDFs of the working and permissible stresses for girder L1, whereas Fig. 3(c) and 3(d) show the PDFs of the working and permissible static stress and deflection for girder M2. The shape of the obtained probability densities reveals again the Gaussian-like distribution of the output metric. The level of overlapping between the working metric and the permissible one shows clearly the performing of the design constraints (see Fig. 3(a), 3(c) and 3(d)). For a case of fatigue stress constraint in Fig. 3(b), the non-overlapping or a large distance between two PDFs shows clearly the fulfillment on this constraint (see also Table 4 for relevant columns with $P_f = 0$ and $\beta = +\infty$ for all girder configurations).

Table 4 presents the probability of failure and reliability index with three independent limit functions. In general, for girders (i.e., L1, M1, H1 named group C1) made up of low yield steels, $Y_s = 230$ N/mm$^2$, it seems that only the static stress constraint works (C1). In the contrary, we need to consider the limit state function based on the static deflection constraint for all remaining girders named group C3 with a high yield stress, $Y_s = 355/450$ N/mm$^2$. In detail, for crane girders of the group C1 the probability of failure varies from 0.0052 to 0.0129 (as decreasing in the reliability index from 2.8676 to 2.2284). In addition, girder designs in the group C3 show the good configuration L2 with $P_f = 0.0002$ (as $\beta \sim 3.5$) and the poor configuration H2 with $P_f = 0.0099$ (as $\beta \sim 2.3$).

Next, we investigate the probability of failure of girder designs with two different coefficients, $COV_F = 0.05$ and $COV_F = 0.1$. In order to reduce the probability of failure of girder design, the geometric factor $k_{geo}$ is tuned from 1.0 to 1.1 and all $COV_{geo}$ are kept at 0.025. The results shown in Fig. 4 indicate that girders of group C1 and C3 are related to the corresponding calculated constraints as stated previously. For only a wheel load $COV_F$ of 0.05 and geometric dimension $COV_{geo}$ of 0.025, the means of geometry parameters have to be larger than 1.1 their deterministic-based values in order to reach a probability of failure at a level of $10^{-4}$. For $COV_F$ of 0.1, it is seen that girders having a factor $k_{geo} = 1.1$ is only enough for a very high level of failure probability ($P_f \sim 0.1$, see lines with

Table 1. Steel yield stress and optimum geometric parameters $x^{op}$ of girders [3]

| Girder | $Y_s$ (N/mm$^2$) | $h^{op}$(mm) | $t_w^{op}$ (mm) | $b^{op}$ (mm) | $t_f^{op}$ (mm) |
|--------|------------------|--------------|-----------------|---------------|-----------------|
| L1 | 230 | 1050 | 6 | 400 | 14 |
| L2 | 355 | 950 | 5 | 375 | 14 |
| L3 | 450 | 1050 | 5 | 375 | 10 |
| M1 | 230 | 1150 | 7 | 375 | 14 |
| M2 | 355 | 1050 | 5 | 325 | 14 |
| M3 | 450 | 1000 | 5 | 325 | 14 |
| H1 | 230 | 1150 | 6 | 450 | 18 |
| H2 | 355 | 1000 | 5 | 325 | 14 |
| H3 | 450 | 1050 | 5 | 425 | 14 |

Table 2. Parameters of considered girders with different working states [3]

| State of loading | $K_p$ | $\bar{w}_p$ | $N_G$ | $\alpha_d$ | $\psi_d$ | $\bar{\sigma}_f$ (N/mm$^2$) |
|---|---|---|---|---|---|---|
| Light (*L*) | 0.50 | *L*/500 | $0.5 \times 10^6$ | 1.00 | 1.1 | $169 + 145(f_\sigma - 0.1)$ |
| Moderate (*M*) | 0.63 | *L*/600 | $1.0 \times 10^6$ | 0.95 | 1.3 | $155 + 135(f_\sigma - 0.1)$ |
| Heavy (*H*) | 0.80 | *L*/700 | $2.0 \times 10^6$ | 0.90 | 1.4 | $142 + 125(f_\sigma - 0.1)$ |

Table 3. Probability statistics of the working stresses and deflection

| Girder | Static stress, $\sigma_s$ (N/mm$^2$) | | | | Fatigue stress, $\sigma_f$ (N/mm$^2$) | | | | Static deflection, $w_p$ (mm) | | | |
|---|---|---|---|---|---|---|---|---|---|---|---|---|
| | *E* | *D* | *Sk* (-) | *Ku* (-) | *E* | *D* | *Sk* (-) | *Ku* (-) | *E* | *D* | *Sk* (-) | *Ku* (-) |
| L1 | 111.1 | 5.0 | 0.15 | 3.05 | 81.9 | 3.2 | 0.15 | 3.06 | 25.5 | 1.9 | 0.24 | 3.12 |
| L2 | 134.9 | 6.1 | 0.16 | 3.05 | 97.9 | 3.9 | 0.16 | 3.05 | 34.8 | 2.6 | 0.24 | 3.11 |
| L3 | 148.3 | 6.9 | 0.16 | 3.05 | 107.4 | 4.4 | 0.16 | 3.05 | 35.8 | 2.7 | 0.24 | 3.11 |
| M1 | 110.4 | 5.1 | 0.16 | 3.05 | 87.8 | 3.6 | 0.16 | 3.05 | 20.7 | 1.6 | 0.24 | 3.11 |
| M2 | 140.4 | 6.5 | 0.15 | 3.04 | 111.0 | 4.7 | 0.16 | 3.04 | 29.4 | 2.2 | 0.24 | 3.11 |
| M3 | 142.9 | 6.6 | 0.16 | 3.04 | 113.2 | 4.8 | 0.16 | 3.04 | 31.0 | 2.3 | 0.24 | 3.11 |
| H1 | 102.1 | 4.7 | 0.15 | 3.05 | 90.4 | 4.0 | 0.15 | 3.05 | 18.4 | 1.4 | 0.24 | 3.11 |
| H2 | 133.0 | 6.1 | 0.15 | 3.04 | 117.8 | 5.2 | 0.16 | 3.05 | 27.1 | 2.0 | 0.24 | 3.11 |
| H3 | 126.5 | 6.0 | 0.15 | 3.04 | 111.6 | 5.0 | 0.15 | 3.04 | 25.4 | 1.9 | 0.24 | 3.10 |
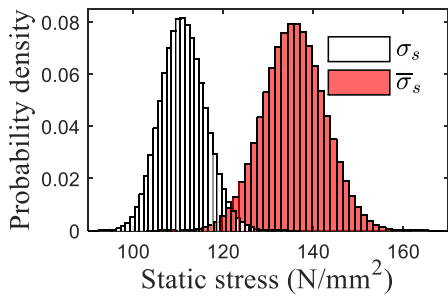


(a) Constraint $G_1$
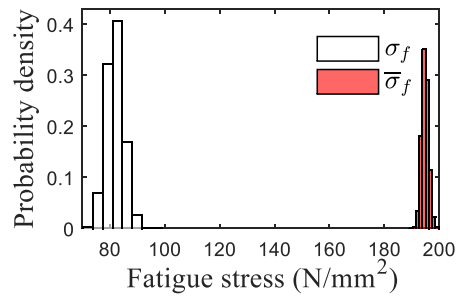
(b) Constraint $G_2$
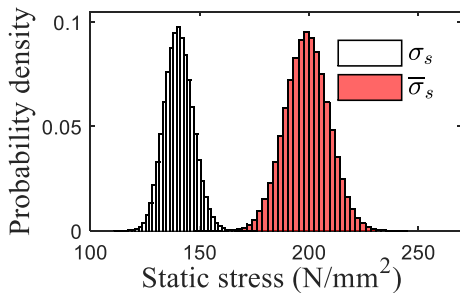
(c) Constraint $G_3$
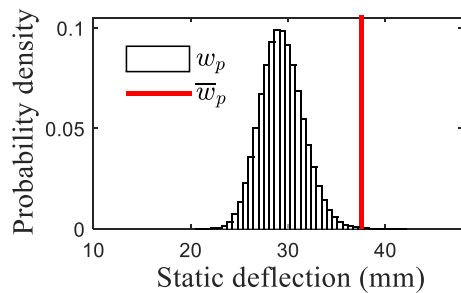
(d) Constraint $G_4$

Figure 3. Probability density of the working and permissible factors for girder L1 (a, b) and girder M2 (c, d)

Table 4. Results of failure probability and the corresponding reliability index

| Girder | Static stress | | Fatigue stress | | Static deflection | |
|--------|------|------|------|------|------|------|
| | $P_f$ | $\beta$ | $P_f$ | $\beta$ | $P_f$ | $\beta$ |
| L1 | 0.0021 | 2.8676 | 0 | $+\infty$ | 0 | $+\infty$ |
| L2 | 0 | $+\infty$ | 0 | $+\infty$ | 0.0002 | 3.4973 |
| L3 | 0 | $+\infty$ | 0 | $+\infty$ | 0.0011 | 3.0615 |
| M1 | 0.0129 | 2.2284 | 0 | $+\infty$ | 0 | $+\infty$ |
| M2 | $2 \times 10^{-6}$ | 4.6114 | 0 | $+\infty$ | 0.0005 | 3.2945 |
| M3 | 0 | $+\infty$ | 0 | $+\infty$ | 0.0046 | 2.6038 |
| H1 | 0.0052 | 2.5646 | 0 | $+\infty$ | 0 | $+\infty$ |
| H2 | $2 \times 10^{-6}$ | 4.6114 | 0 | $+\infty$ | 0.0099 | 2.3291 |
| H3 | 0 | $+\infty$ | 0 | $+\infty$ | 0.0007 | 3.1841 |

circle markers in Fig. 4(a)).



(a) Constraint $G_1$      (b) Constraint $G_2$
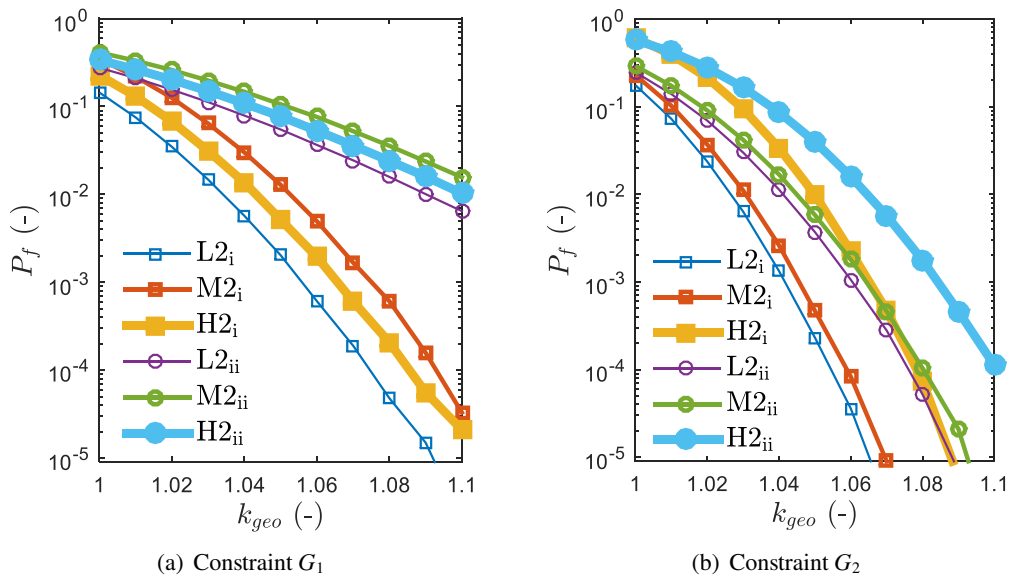
Figure 4. Probability of failure (in semilogarithmic scale) of girders with $COV_F = 0.05$
(squares and legends with subscripts i) and $COV_F = 0.1$ (circles and legends with subscripts ii):
the static stress constraint (a), and the deflection constraint (b)

## 5. Conclusions

This paper focuses on estimating the failure probability of overhead crane bridge girders with uncertain design parameters. Monte Carlo approach is utilized to quantify the effect of the uncertainties of design parameters on the failure probability with several limit state functions constructed from a set of selected design constraints. From the obtained results, the following concluding remarks can be stated:

(i) For the considered normal distribution, all output metrics including maximum stress and deflection tend to have the same distribution function in compared with the input uncertain variables.

(ii) By increasing the geometric factor from $k_{geo} = 1$ to $k_{geo} = 1.1$, we can make the deterministic-based designs with a low reliability ($P_f \sim 0.5$) to reliability-based designs with a very low failure probability ($\sim 10^{-4}$) for a case of COV $< 0.05$.

(iii) For high strength steels ($Y_s > 355$ N/mm$^2$) the deflection constraint should be considered only, whereas for low strength steels ($Y_s < 230$ N/mm$^2$) it is required to check the constraint on static stress. Having $P_f = 0$ for all girder configurations, this means that the constraint fatigue stress can be neglected.

Finally, it is obvious that uncertain design parameters lead to the failure probability of crane girders, but a reliability and sensitivity analysis of a crane girder involving parameters of its building frame [23] should be conducted in forthcoming works for reaching reliability-based designs in real applications.

# References

[1] Hong, K.-S., Shah, U. H. (2019). *Dynamics and control of industrial cranes*. Springer.

[2] Verschoof, I. J. (2002). *Cranes: design, practice, and maintenance*. Wiley-Blackwell.

[3] Farkas, J. (1986). Economy of higher-strength steels in overhead travelling cranes with double-box girders. *Journal of Constructional Steel Research*, 6(4):285–301.

[4] Rao, S. S. (1978). Optimum design of bridge girders for electric overhead traveling cranes. *Journal of Engineering for Industry*, 100(3):375–382.

[5] Liu, P. F., Xing, L. J., Liu, Y. L., Zheng, J. Y. (2014). Strength analysis and optimal design for main girder of double-trolley overhead traveling crane using finite element method. *Journal of Failure Analysis and Prevention*, 14(1):76–86.

[6] Pinca, C. B., Tirian, G. O., Socalici, A. V., Ardeleadn, D. E. (2009). Dimensional optimization for the strength structure of a traveling crane. *WSEAS Transactions on Applied and theoretical Mechanics*, 4(4): 147–156.

[7] Tam, C. M., Tong, T. K. L. (2003). GA-ANN model for optimizing the locations of tower crane and supply points for high-rise public housing construction. *Construction Management and Economics*, 21 (3):257–266.

[8] Lagaros, N. D., Papadrakakis, M. (2012). Applied soft computing for optimum design of structures. *Structural and Multidisciplinary Optimization*, 45(6):787–799.

[9] Mijailović, R., Kastratović, G. (2009). Cross-section optimization of tower crane lattice boom. *Meccanica*, 44(5):599.

[10] Gašić, M. M., Savković, M. M., Bulatović, R. R., Petrović, R. S. (2011). Optimization of a pentagonal cross section of the truck crane boom using Lagrange's multipliers and differential evolution algorithm. *Meccanica*, 46(4):845–853.

[11] Jármai, K. (1990). Decision support system on IBM PC for design of economic steel structures applied to crane girders. *Thin-Walled Structures*, 10(2):143–159.

[12] Sun, C., Tan, Y., Zeng, J., Pan, J.-S., Tao, Y. (2011). The structure optimization of main beam for bridge crane based on an improved PSO. *Journal of Computers*, 6(8):1585–1590.

[13] Sun, G., Li, G., Zhou, S., Li, H., Hou, S., Li, Q. (2011). Crashworthiness design of vehicle by using multiobjective robust optimization. *Structural and Multidisciplinary Optimization*, 44(1):99–110.

[14] Lagaros, N. D., Plevris, V., Papadrakakis, M. (2010). Neurocomputing strategies for solving reliability-robust design optimization problems. *Engineering Computations*, 27(7):819–840.

[15] Fan, X., Bi, X. (2015). Reliability-based design optimization for crane metallic structure using ACO and AFOSM based on China standards. *Mathematical Problems in Engineering*, 2015:1–12.

[16] Yu, L., Cao, Y., Chong, Q., Wu, X. (2011). Reliability-based design for the structure of tower crane

under aleatory and epistemic uncertainties. In *2011 International Conference on Quality, Reliability, Risk, Maintenance, and Safety Engineering*, IEEE, 938–943.

[17] Meng, W., Yang, Z., Qi, X., Cai, J. (2013). Reliability analysis-based numerical calculation of metal structure of bridge crane. *Mathematical Problems in Engineering*, 2013:1–5.

[18] Ditlevsen, O., Madsen, H. O. (1996). *Structural reliability methods*. Wiley, Chichester, UK.

[19] Duong, B., van Gelder, P. (2016). Calibrating resistance factors under load and resistance factor design method (LRFD) using Monte-Carlo simulation. *Journal of Science and Technology in Civil Engineering (STCE)-NUCE*, 10(5):79–87.

[20] Hu, C., Youn, B. D., Wang, P. (2019). *Engineering design under uncertainty and health prognostics*. Springer.

[21] Zio, E. (2013). System reliability and risk analysis. In *The Monte Carlo simulation method for system reliability and risk analysis*, Springer, 7–17.

[22] British Standards Institution, BS 2573 (1983). *Part I, Rules for the design of cranes, specification for classification, stress calculations and design criteria for structures*. London, BSI.

[23] Thuat, D. V., Chuong, H. V., Hoa, N. D. (2017). Evaluation of lateral static earthquake and wind loads applied on one-story industrial steel building frames with cranes. *Journal of Science and Technology in Civil Engineering (STCE)-NUCE*, 11(1):11–18. (in Vietnamese).